UNIVERSITI PUTRA MALAYSIA

QUANTIFICATION OF NEURONAL MORPHOLOGY AND MATURATION OF N2a CELLS USING NEURPHOLOGYJ SOFTWARE

DOREEN MARIA A/P ANTHONYSAMY

lp
FPSK2 2020 41

QUANTIFICATION OF NEURONAL MORPHOLOGY AND MATURATION OF N2a CELLS USING NEURPHOLOGYJ SOFTWARE

BY

DOREEN MARIA A/P ANTHONYSAMY

A PROJECT PAPER SUBMITTED AS PARTIAL REQUIREMENT FOR THE DEGREE OF BACHELOR OF SCIENCE (BIOMEDICAL SCIENCES)

DEPARTMENT OF BIOMEDICAL SCIENCE
FACULTY OF MEDICINE AND HEALTH SCIENCES
UNIVERSITI PUTRA MALAYSIA
SERDANG, SELANGOR

2020

© COPYRIGHT UPM

QUANTIFICATION OF NEURONAL MORPHOLOGY AND MATURATION OF N2a CELLS USING NEURPHOLOGYJ SOFTWARE

Doreen Maria Anthonysamy[a], Cheah Yoke Kqueen[a], Sharmili Vidyadaran[b]

[a]*Department of Biomedical Sciences, Faculty of Medicine and Health Sciences, Universiti Putra Malaysia, Serdang, Malaysia*

[b]*Department of Pathology, Faculty of Medicine and Health Sciences, Universiti Putra Malaysia, Serdang, Malaysia*

ABSTRACT

N2a is a cell line used widely in studies of neuronal maturation and development in mouse neuroblastoma. Growth of N2a cells via its differentiation into mature neurons is traditionally induced by serum deprivation (SD) method as serum has been known to contain inhibitory factors that may impede neuronal differentiation and neurite growth. Even though that soma count and neurite length, amongst other neuronal features of differentiated N2a cells, can be efficiently-analyzed using various open-source tools and software, the use of NeurphologyJ software to characterise and examine the morphological features of N2a cell has not been explored within the neuroinflammation group. To measure neuronal morphology parameters (soma count, neurite length, neurite count, attachment point and endpoints) of undifferentiated and differentiated N2a cells using NeurphologyJ software. N2a cells were maintained in 0.5% fetal bovine serum at 37°C in DMEM supplemented and 5% CO_2 incubation conditions and were stained with FITC-labelled neuron-specific class III beta-tubulin (Tuj1) marker and 4′,6-Diamidino-2-Phenylindole (DAPI), prior viewing under a fluorescent microscope. The cell culture was conducted by another colleague. Captured images were processed using a fluorescent imaging system, converted to TIFF file format, and were digitally-enhanced before evaluation using NeurphologyJ software. Optimal threshold levels were set individually for each parameter, prior features extraction and determination. These features include neurite length, attachment point, neurite count, endpoints, and soma count. The differences between undifferentiated and differentiated N2a cells were analyzed using the Mann–Whitney test. It was determined that differentiated cells when compared with undifferentiated cells, represent significantly (p<0.05) higher counts of soma (161.33±64.96 vs 88.50±23.81), neurite count (2362±605.43 vs 772.00±248.01), neurite length (2348.67±1345.79 vs 18451.33±7963.13), attachment points (995.67±295.88 vs 185.83±90.95), and endpoints (1383±622.28 vs 166.33±85.77). These findings suggest that NeurphologyJ software can be useful for the measurement of morphological features of both undifferentiated and differentiated N2a cells. For future applications, N2a cells differentiated using other types of methods may be conducted for a better understanding of cell maturation parameters. Other than that, a comparison of N2a cells with other neuronal cell lines by measuring the parameters using NeurphologyJ software can also be conducted.

© COPYRIGHT UPM

Keywords: N2a cell; neurite outgrowth; NeurphologyJ; neuronal differentiation; serum deprivation.

© COPYRIGHT UPM

KUANTIFIKASI MORFOLOGI NEURONAL DAN MATURASI SEL N2a MENGGUNAKAN PERISIAN NEURPHOLOGYJ

Doreen Maria Anthonysamy[a], Cheah Yoke Kqueen[a], Sharmili Vidyadaran[b]

[a]*Jabatan Sains Biomedikal, Fakulti Perubatan dan Sains Kesihatan, Universiti Putra Malaysia, Serdang, Malaysia*

[b]*Jabatan Patologi, Fakulti Perubatan dan Sains Kesihatan, Universiti Putra Malaysia, Serdang, Malaysia*

ABSTRAK

N2a adalah garis sel yang digunakan secara meluas dalam kajian pematangan dan perkembangan neuron pada neuroblastoma tikus..Pertumbuhan sel N2a melalui pembezaannya menjadi neuron matang secara tradisional disebabkan oleh kaedah kekurangan serum (SD) kerana serum telah diketahui mengandungi faktor penghambat yang dapat menghalang pembezaan neuron dan pertumbuhan neurit. Walaupun fakta bahawa bilangan soma dan panjang neurit, antara ciri neuron sel N2a yang berbeza, dapat dianalisis dengan berkesan menggunakan pelbagai alat dan perisian sumber terbuka, penggunaan perisian NeurphologyJ untuk mencirikan dan memeriksa ciri morfologi sel N2a belum telah diterokai dalam kumpulan radang saraf. **Objektif:** Untuk mengukur parameter morfologi neuron (kiraan soma, panjang neurit, kiraan neurit, titik lampiran dan titik akhir) sel N2a yang tidak dibezakan dan dibezakan menggunakan perisian NeurphologyJ. Sel N2a dikekalkan dalam DMEM ditambah dengan serum sapi janin 0.5% pada suhu 37 ° C dan 5% keadaan inkubasi CO2 dan diwarnai dengan penanda beta-tubulin kelas III berlabel FITC (Tuj1) dan 4 ′, 6-Diamidino- 2-Phenylindole (DAPI), sebelum melihat di bawah mikroskop pendarfluor. Pembudayaan sel dilakukan oleh pelajar pascasiswazah. Gambar yang dirakam diproses menggunakan sistem pencitraan neon, diubah ke format file TIFF, dan ditingkatkan secara digital sebelum dinilai menggunakan perisian NeurphologyJ. Tahap ambang optimum ditetapkan secara individu untuk setiap parameter, pengekstrakan dan penentuan ciri sebelumnya. Ciri-ciri ini merangkumi panjang neurit, titik lampiran, kiraan neurit, titik akhir, dan kiraan soma. Perbezaan antara sel N2a yang tidak dibezakan dan dibezakan dianalisis menggunakan ujian Mann-Whitney. Telah ditentukan bahawa sel yang dibezakan jika dibandingkan dengan sel yang tidak dibezakan, mewakili jumlah soma yang lebih tinggi ($p < 0.05$) (161.33 ± 64.96 vs 88.50 ± 23.81), jumlah neurit (2362 ± 605.43 vs 772.00 ± 248.01), panjang neurit (2348.67 ± 1345.79 vs 18451.33 ± 7963.13), titik lampiran (995.67 ± 295.88 vs 185.83 ± 90.95), dan titik akhir (1383 ± 622.28 vs 166.33 ± 85.77). Penemuan ini menunjukkan bahawa perisian NeurphologyJ dapat berguna untuk pengukuran ciri morfologi kedua-dua sel N2a yang tidak dibezakan dan dibezakan. Untuk aplikasi masa depan, sel N2a yang dibezakan menggunakan jenis kaedah lain dapat dilakukan untuk pemahaman yang lebih baik mengenai parameter pematangan sel. Selain itu, perbandingan sel N2a dengan garis sel neuron lain dengan mengukur parameter menggunakan perisian NeurphologyJ juga dapat dilakukan.

© COPYRIGHT UPM

Kata kunci: Sel N2a; pertumbuhan neurit; NeurphologyJ; pembezaan neuron; kekurangan serum.

© COPYRIGHT UPM

ACKNOWLEDGEMENT

First of all, I would like to thank The All-Powerful God for enabling me to complete this research. I wish to express my sincere thanks to my research supervisor Y. Bhg. Professor Dr. Cheah Yoke Kqueen and Assoc. Prof. Dr. Sharmili Vidyadaran for giving me the opportunity to conduct research and for providing invaluable guidance throughout. Thank you, Assoc. Prof. Dr. Sharmili Vidyadaran, for her dynamism, vision, sincerity and motivation have deeply inspired me. She has thought me the methodology to carry out the research and to present the research work as clear as possible. It was a great privilege and honour to work and study under her guidance.

My sincere appreciation for the excitement and assistance of my lab in providing important help and motivation to complete this thesis. Thanks to (Siti Sarah, Lily, Vivek, Shamin, Omar and Aini) for the great energy and friendship. Most importantly, feeling grateful to supportive staff (Mr. Anthonysamy, Aishah, and Marsitah), for their assistance in documenting the operation of laboratory equipment, and authoritative administrative work. I am obliged to share with each of you, for your steady help and eagerness, the information from which I have adapted to this extent. I owe my gratitude and reverence to my noble parents for their relentless moral guidance and mellifluous love that enabled me to excel in everything and without their loving devotion, this thesis would have been a mere vision. Through this study it is the goodness of those known people that see the light of day.

© COPYRIGHT UPM

Table of Contents

	Page
ABSTRACT	**ii**
ABSTRAK	**iv**
ACKNOWLEDGEMENT	**vi**
APPROVAL	**vii**
DECLARATION	**viii**
LIST OF FIGURES	**xi**
LIST OF ABBREVIATION	**xiii**
CHAPTER	
1.0 INTRODUCTION	1
1.2 Problem statement	3
1.3 Objective of the study	3
1.3.1 General objective	3
1.3.2 Specific objective	3
1.4 Research hypothesis	3
2.0 LITERATURE REVIEW	4
2.1 Anatomy of Neurons	4
2.1.1 Morphology of Neurons	5
2.1.2 Neuronal maturation	6
2.2 Neuroblastoma cell line	7
2.3 Immunofluorescence staining	8
2.3.1 Fluorescein-5-isothiocyanate (FITC)	9
2.3.2 4′,6-diamidino-2-phenylindole (DAPI)	10
2.4 Immunofluorescent microscope	10
2.5 Application of ImageJ	11
2.5.1 NeurphologyJ	12
2.5.2 Neuronal parameters	13
3.0 MATERIAL AND METHODOLOGY	14
3.1 Cell culture maintenance	15
3.1.1 Maintaining cell lines	15
3.1.2 Cell subculturing	15
3.3 Immunofluorescence staining	16
3.4 Fluorescent microscopy	17
3.5 Neurphology J	18
3.5.1 Installation instruction	18
3.5.2 Operation instruction: NeurphologyJ interactive	18
3.6 Statistical analysis	28

© COPYRIGHT UPM

4.0 RESULTS 29
4.1 Fluorescent microscope images 29
4.2 Digital analysis using NeurphologyJ 31

5.0 DISCUSSION 35
6.0 CONCLUSION AND FUTURE RECOMMENDATION 39

REFERENCES 40
APPENDIX A 44

© COPYRIGHT UPM

LIST OF FIGURES

Figure		Page
1.1	Structure of a neuron	18
1.2	N2a cell culture	20
3.1	Summary of methodology	27
3.2	Fluorescent image of N2a cells after uploading in NeurphologyJ	18
3.3	Gray-scale image of N2a cells after conversion using NeurphologyJ	19
3.4	TIFF-formatted, gray-scale image of N2a cells saved	19
3.5	Adjustment of lower and upper selection bars to achieve optimum threshold levels	20
3.6	Output image of N2a cells after optimal threshold adjustment	21
3.7	Adjustment of lower and upper selection bars to achieve optimum soma threshold levels	22
3.8	Adjustment of the contrast level	23
3.9	Adjustment of the soma intensity	24
3.10	Adjustment of neurite width	24
3.11	Adjustment of particle clean up value.	25
3.12	Adjustment of proper threshold selection values	25
3.13	Summary table of output from NeurphologyJ analysis	26
4.1	Immunocytochemical staining of untreated N2a cells as control	42
4.2	Immunocytochemical staining of treated cells N2a with serum deprivation.	43
4.3	Mean soma count in N2a cells	46
4.4	Mean neurite count in N2a cells	46

© COPYRIGHT UPM

Figure		Page
4.5	Mean neurite length in N2a cells	47
4.6	Mean attachment point in N2a cells	47
4.7	Mean endpoint point in N2a cells	48

© COPYRIGHT UPM

LIST OF ABBREVIATION

2D	Two dimensional
ATCC	American type culture collection
BSA	Bovine serum albumin
CO_2	Carbon dioxide
DAPI	4′,6-diamidino-2-phenylindole
DMEM	Dulbecco's updated minimum essential medium
EDTA	Ethylenediamine tetraacetic acid
FBS	Fetal bovine serum
FITC	Fluorescein-5-isothiocyanate
N2a	Neuroblastoma
PFA	Paraformaldehyde
T75	Thermo scientific™ Nunc™ non-treated flasks
TUJ1	Neuron-specific class III beta-tubulin

© COPYRIGHT UPM

CHAPTER 1

INTRODUCTION

The ability of the molecules in culture to cause neurite outgrowth is the hallmark test used for assessing neurotrophic activity. Photographs are traditionally processed manually, using labour-intensive, time-consuming, and error-prone techniques. While systems are available commercially for fully automated neurite screens, some aren't well documented. Most of the published neurite outgrowth measurements are still being performed with the research type's minimally automated image analysers. Although flexible, these research image analyzers are highly interactive, with very low throughput, and poorly validated by screening assays. Neurite outgrowths in culture are used to evaluate neurotrophic activity. Neurite measurements were performed very slowly using manual methods, or more efficiently with digital image analysis systems. By contrast, the analyzes of the medium-throughput and non-interactive images from neurite screens were not well established. Cell screening requires automation at walk-away. Neurite measurements were carried out very slowly using manual processes, or with digital image analysis systems more effectively. By comparison, neurite screens analysis of the medium-throughput and non-interactive image was not well defined. Cell screening requires walk-away automation.

© COPYRIGHT UPM

The key challenge for automation is the isolation of appropriate neurite material from other cellular materials, without human interference. The computer must determine when a protuberance of a cell body is a neurite, and when it is just a protuberance. The artefacts must be disregarded and robustly function through medical environments and cell type. Due to the complexity of the decisions involved, automated analyzes can be far more vulnerable to error than human scoring, and may lack the ability to identify treatment results that would be found in manually scored samples So, verification of any automated device is important. A viable screening device could operate, as well as a human operator, but could be much faster. That is, the automated device must be able to extract neurites and only neurites from a complex picture and display error variance that approximates the collected manually. These characteristics must be maintained across the spectrum of conditions found in standard assays and without more complicated and costly staining procedures being needed.

© COPYRIGHT UPM

1.2 Problem Statement

The use of NeurphologyJ software to characterise and examine the morphological features of N2a cells has not been explored within the neuroinflammation group.

1.3 Objective of the Study

1.3.1 General Objective

To assess NeurphologyJ software for characterisation of N2a cells maturation by comparing the neurite outgrowth and complexity.

1.3.2 Specific Objective

a) To measure neuronal morphology parameters (soma count, neurite length, neurite count, attachment point and endpoints) of N2a cells using NeurphologyJ software.

b) To compare the morphological differences between undifferentiated and differentiated N2a cell line based on the morphological parameters.

1.4 Research Hypothesis

NeurphologyJ software can be used to study the morphological characteristics of N2a cells such as soma count, neurite count, neurite length, attachment point and endpoints.

© COPYRIGHT UPM

CHAPTER 2

LITERATURE REVIEW

2.1 Anatomy of Neurons

Neurons are the nervous system's fundamental unit, and specialized cell. Nearly all cells contained neurons in the nervous system. Cells within the developing brain are experiencing a growth period that involves everything. Initially, a neuronal progenitor cell travels to the appropriate location within the brain and eventually expands long expansions that are the axon and dendrites used by the neuron formed to speak to various cells. The neurotransmitters need to be determined which neurons interface with various neurons (Radio *et al.,* 2008). The role of the nervous system is to detect surroundings and respond to them. Major parts of the peripheral nervous system, and of the central nervous system. Neurons send, receive and share information from all parts of the body. Neurons are nervous system components. Neurons receive signals and transmit them to different parts of the body. Both physically and electrically this is achieved (Barnes *et al.,* 2009). There are several different types of neurons that facilitate the transmission of information. The sensory neurons bring input into the brain from the sensory receptor cells that are located inside the body. The motor neurons, when transmitting muscle input from the brain. The interneurons relay information between the various neurons throughout the body. Numerous components are required to ensure the proteins involved in this process are identified when and where it occur.

© COPYRIGHT UPM

2.1.1 Morphology of Neurons

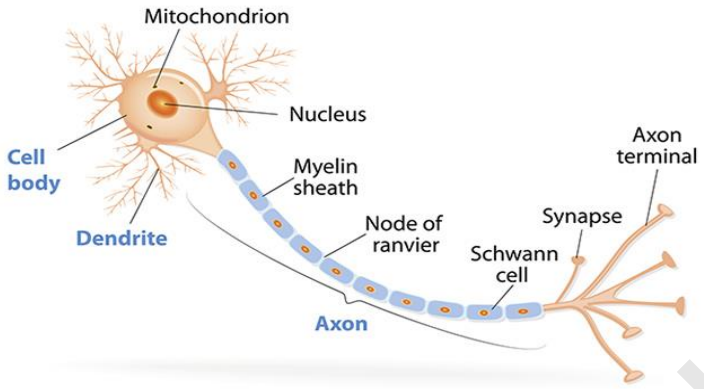

Figure 1.1: Structure of a neuron.
Source: https://qbi.uq.edu.au/brain/brain-anatomy/axons-cable-transmission-neurons

Neuron consists of a synaptic, cell body process (Figure 1.1). Neurons are among the most entranced forms of cells in the body and are split into two molecular regions, the axon and the dendrites being undeniable for all intents and purposes. Usually, neurons structure a singular axon and various dendrites in the central tangible framework that underlie the directional movement of information move. Dendrites facilitate synaptic data wellsprings, set standards at soma level for duration of operation, multiply along the axon, allowing for presynaptic contacts on target cells. Axons transmit signals from the phone body, consisting of long nerve types imparting signs to specific territories. Neurotransmitters are classified as end-of-axon intersections (Chen *et al.*, 2020). Axons are covered with myelin sheaths, which helps to keep electrical signals flowing rapidly in the cell. Dendrites, impart signs to the cell body and shorter, contrasted with axons additionally spreading. Specific neurotransmitters present in dendrites for collecting signals from surrounding neurons.

© COPYRIGHT UPM

2.1.2 Neuronal maturation

Neurons are a part in which, represents fundamental on the intersections and terminations, usually referred to as basic focuses, making the proper restriction and clear evidence of such a critical recreational undertaking. Considering the major differences between existing and juvenile neuronal societies, growing physiological importance, one of the problems nowadays is to identify on impacts of mixes which strongly associates and separate neuron. Neurons have a deeply spellbound structure that fits the vectorial data stream. We usually have a few dendrites that receive presynaptic neuronal inputs and one axon that passes data to post-synaptic neurons (Ramm *et. al.,* 2003). Neurites are tube-shaped distensions that include a developmental cone at their distal tip, and require axonal or dendritic procedures to acquire sub-atomic and basic attributes. Without net lengthening these neurites extend and withdraw. A few days after the fact, the remaining neurites develop and branch to frame the dendrites and the axons and dendrites begin to grow and dendritic distensions or spines appear in the last advance of growth (West *et. al.*, 2011).

© COPYRIGHT UPM

2.2 Neuroblastoma cell line

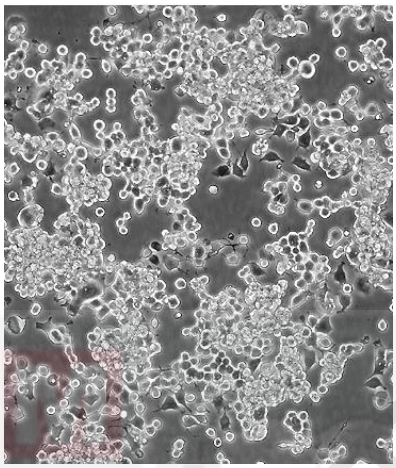

Figure 1.2: N2a cell culture.
Source: https://www.atcc.org/products/all/CCL-131.aspx/#characteristics

Neuro 2A (N2a) is a mouse cell line derived neural peak commonly used for investigating neuronal separation, axonal growth, and flagging pathways. The ability to deliver neuronal cell communities in vitro was critical in propelling the functioning of the sensory system. Neuronal cells development is checked because neurons grow do not undergo cell division (Figure 1.2). One approach to overcome this is to create optional cell lines that have been obtained and deified from neuronal tumours (Merhie *et al.*, 2019). These have the advantage of having the choice to offer boundless cell numbers in a relatively effective way in cell culture.

N2a may be completely distinct from neurons and their separation is usually acquired directly from refined conditions, such as serum deficiency to form of lifestyle. Their tendency to divide into neurons can be calculated not only by the general subjective cell morphology evolving around the soma, but also by the number and length of the neurite as expansions (Mitra *et al.*, 2013).

© COPYRIGHT UPM

2.3 Immunofluorescence staining

Tagging approaches using fluorophores promote the specific representation of biomolecules, complex cell types, organelles, the conduct of single cells and cell populations, organogenesis, and even the advancement of fixed and living examples of life forms. Fluorophore-based naming approaches are usually based on direct contact with biomolecules, engineered fluorescent stains and experiments, or immunofluorescence-(IF) restricting counteracting agent antigen. Typically, synthetic fluorescent stains and experiments are applied to fixed cells or tissues. Cell porousness of the applied manufactured fluorescent stain should be considered, for live imagery draws close. Fluorescent stains the most widely used use dyes to explicitly stain nucleic acids, cell structures. The selectivity of IF recolouring techniques is provided by the reaction of an essential neutralizer raised against a particular antigen of intrigue. Numerous auxiliary antibodies that coupled to an engineered fluorescent colour then concentrate on each critical immunizer. Due to this enhancement of the symbol, IF provides unrivalled differentiation of example. Then again, with fluorophores diminishing foundation recolouring and the term of the recolouring mechanism, important antibodies may be legitimately called. In case that makes an amazing degree of adaptability in choosing manufactured colours that are fluorescent at various wavelengths and can be paired with other cell segments being specifically identified.

© COPYRIGHT UPM

2.3.1 Fluorescein-5-isothiocyanate (FITC)

Fluorescein-5-isothiocyanate (FITC) is a fluorescent light and has a location with the colours of xanthenes. The FITC is used for the naming of various biomolecules. Immunoglobulins, lectins, and specific proteins, peptides, nucleic acids and nucleotides; for example, oligo- and polysaccharides. Fluorescein-5-isothiocyanate (FITC) is a fluorescent light and has a place with xanthene colors. The FITC is used for the naming of various biomolecules. For example, immunoglobulins, lectins, and different proteins, peptides, nucleic acids, nucleotides; oligo- and polysaccharides. Since of their high absorptivity, excellent quantum yield of fluorescence, and great solvency of water, fluorescein subordinates are the most well-known fluorescent reagents for natural analysis. Fluorescein-based colors and their conjugates have a few qualities of presentation which may promote or include use in different applications. Fluorescein displays a relatively high rate of fluorescent photobleaching that is touchy to pH changes (Wu *et al.*, 2016). A moderately wide range of fluorescence emanation, extinguishing fluorescence upon conjugation with biopolymers. The broad fluorescein spectrum blends and branches much like a succession of superior fluorophores with better labelling and position attributes.

© COPYRIGHT UPM

2.3.2 4′,6-diamidino-2-phenylindole (DAPI)

A simple-to-use fluorescent stain, 4′,6-diamidino-2-phenylindole (DAPI), imagines atomic DNA both in living cells and in fixed cells. DAPI recolouring was used to determine the number of cores and survey the net cell morphology. The recoloured cells were prepared for electron microscopy after light minuscule investigations (Saroa *et al.,* 2018). Cells recoloured with DAPI display no ultrastructural changes in comparison to cells not recoloured with DAPI. DAPI recolouring allows different use of cells that dispense with the copy test requirement (Djouhri *et al.,* 2020). It is often routinely used to test cells, predict apoptosis, Organize DNA-based cells, and as an atomic division tool in high-content imaging science, given its high DNA like. DAPI is widely used to recolour fixed cells because the colour is impermeable to the cells, given the fact that the stain can reach live cells when used at higher fixations.

2.4 Immunofluorescent microscope

A lens that magnifies fluorescence is an optical magnifying lens that uses fluorescence to recognize the properties of natural or inorganic compounds rather than ignore, disperse, reflect, and weaken or retain. Fluorescence magnifying device refers to any magnifying device that uses fluorescence to create a picture, regardless of whether it is a more basic setup such as an epifluorescence magnifying device or a more muddled structure, such as a confocal magnifying device that uses optical segmentation to show signs of improvement of the fluorescence picture (Pu *et al.,* 2020). The example is illuminated by the light of a specific frequency consumed by

© COPYRIGHT UPM

the fluorophores, which causes them to radiate longer frequencies. Using a different worldly outflow channel, the enlightenment light is isolated from much more fragile transmitted fluorescence. The feasible use of this technique requires several considerations, including the antigen concept, specific immune response, permeabilization and fixation, and cell fluorescence imaging. Although it may require fine tuning of the protocol depending on the type of cell, the neutralizer and the antigen, simple steps are feasible for all applications.

2.5 Application of ImageJ

Open-source programming is ideal for scientists because it can be analyzed, altered and redistributed without reservation; in particular, the ImageJ open-programming process has greatly influenced the sciences of life and continues to do so (Schindelin *et al.,* 2015). ImageJ has emerged entirely from its roots due to being largely publicly accessible and its active and welcoming client network. ImageJ employments range from the portrayal of information and instruction to specialized image handling and accurate inquiry. In this review, we use the ImageJ venture as a theoretical analysis into how open-source programming cultivates its programming instrument sets, making vast quantities into creativity in picture evaluation easily available to conventional researchers. We examine specifically what makes ImageJ so popular, how it affects the sciences of life, how it motivates various tasks and how it is influenced by coevolving projects within the ImageJ community (Rueden *et al.,* 2017). Given the fact that ImageJ was at first developed for the sciences of life, it is often used in many other rational trains. ImageJ will view two-dimensional planes of an N-dimensional image in a window with sliders to monitor which plane is obvious.

© COPYRIGHT UPM

2.5.1 NeurphologyJ

The evaluation of the use of ImageJ (NIH) with the NeurphologyJ module, a multi-faceted type of neuron morphology, including soma size, neurite length, and neurite growth. Using ImageJ Free Programming. NeurphologyJ uses requests from ImageJ, and uses a reduced Java modules game program. When supervising unambiguous applications or for possible extensions, being structured as an ImageJ module has the advantage of simple customisation. Instinctive and high-throughput NeurphologyJ is given two transformations. The solid structure helps to raise the limits for the highly variable throughput (Chiola *et al.,* 2019). The NeurphologyJ figure includes five regions, one part of the image update and four parts of the morphological assessment. On pharmacological frustration, NeurphologyJ can discern neuronal morphological changes. Open activity consists of a boundary range, called the n-wide boundary, which rises to the width of the thickest neurite. The calculation of n-width is determined by the Consumer. For example, cell garbage has an additional advantage to this open process when evacuating small debasing posts. The updated picture is subsequently binarized first, and a client-defined scale called the p-size boundary eliminates all phone trash and tiny particles (Ho *et al.,* 2011). The resulting "cleaned" image is skeletonized into one-pixel wide skeletons to thin it out.

© COPYRIGHT UPM

2.5.2 Neuronal parameters

NeurphologyJ is used to measure neuronal traits Such as soma number and size, neurite length and distance, attachment points, and endpoints. To acquire the image introducing neurite length, somata are deduced from the "skeleton" illustration. The length of the neurite is measured using the "Analyze Particles" command to include all pixels in the picture 'neurite range'. The neurite relationship points to being the region where the soma has neurite contact. A wider order with the goal estimates of 1 and the test estimate of 1 is used to expand somata size for focusing on the neurite relation. Closure point, just like the neurite tip region. For extracting only one pixel from a fiber tip, a dissolve order with a focus estimate of 1 and a count estimate of 7 were used. The end pixels of the single-pixel objects in the skeleton image were kept to get neurite finishing attention, and the corresponding pixels that do not converge with the extended soma were named as completion of a solitary image NeurphologyJ can quantify more morphological highlights. For community management, NeurphologyJ uses a dynamic memory assignment where the memory allocated to prepare a picture is provided after the test is done. All the images in an envelope can be examined in one bunch in this manner.

© COPYRIGHT UPM

CHAPTER 3

MATERIAL AND METHODOLOGY

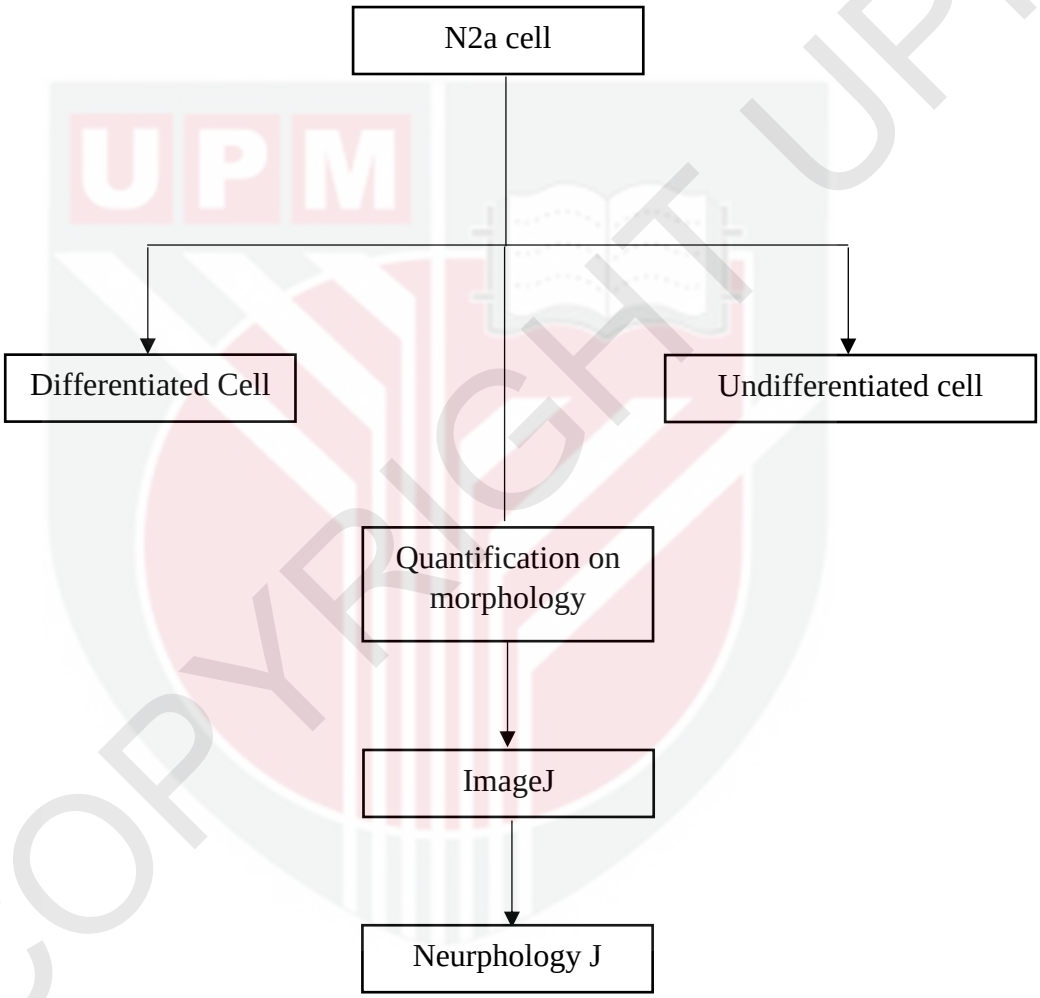

Figure 3.1: Summary of methodology. The methodology is divided into two parts which are N2a cell analysis between undifferentiated and differentiated cells using NeurphologyJ software.

© COPYRIGHT UPM

3.1 Cell culture maintenance

3.1.1 Maintaining cell lines

Neuro-2a mouse neuroblastoma cell line (ATCC, CCL-131) has been maintained as a monolayer culture in Dulbecco's updated Minimum Essential Medium (DMEM) supplemented with 10% fetal bovine serum (FBS), penicillin (100 units/mL) and streptomycin (100 mg/mL). The cells were cultured in a T75 flask at a seeding density of 5 x 10^5 cells/mL and incubated at 37°C, in a humidified environment with 5% CO_2 content.

3.1.2 Cell subculturing

Cells were subcultured when cells have reached a confluency of 80-90%. The old media were discarded from the 75cm^2 culture flask. The cells were then washed twice with 5 mL of 1 x Phosphate Buffered Saline (PBS) to remove all traces of the residual media. About 2 mL of 0.25% trypsin-EDTA were then injected into the flask and incubated for 5 minutes in a 5% CO_2 incubator to release the cells from the flask. Afterward the cells were studied under a microscope to ensure complete cell separation. In the flask, 5 mL of new media was introduced to avoid trypsin action. The mixture was then transferred to a centrifugal tube of 15 mL, followed by centrifugation at 1,200 rpm for 5 minutes. The supernatant was discarded and 5 mL of 1x PBS was used to resuspend the pellet. The mixture was centrifuged at 1,200 rpm for 5 minutes. The supernatant was removed, and 5 mL of media was added, and the

© COPYRIGHT UPM

pellet was gently resuspended. The subculture ratio used was 1:2, so 2.5 mL of the resuspended cells were pipetted into two new flasks.

3.2 N2A differentiation assay

Cells of 90% confluency were washed twice with 5 mL PBS, trypsinised with 2 mL of 0.25% trypsin-EDTA, incubated at 37ºC for 5 minutes, added with 5 mL complete media and centrifuged at 1,200 rpm at room temperature for 5 minutes. For cell harvesting, the cell pellet was washed twice with 5 mL of 1x PBS and to resuspend the pellet, the cells were centrifuged at 1,200 rpm for 5 minutes. The supernatant was removed and the pellet was resuspended in 2 mL media. Coverslips were placed in a 24-well plate followed by the addition of 500 uL of poly L lysine. The plate was gently swirled and incubated at room temperature for 10 minutes. The wells were washed with 1x PBS solution. About 2,500 cells were seeded into the empty wells in 1 mL media. Initially, media with 10% FBS was used. On day 1, the media was replaced with 0.5% FBS-containing media for differentiation induction. The media was replaced every 2 days and the cells were cultured for 8 days.

3.3 Immunofluorescence staining

Supernatant from the cultured well plates was discarded and the cells were rinsed with 1x PBS, incubated in 5% CO_2 incubator for 10 minutes and 20 ug/mL of DAPI stain was applied to the cultures. The supernatant was discarded and the cultures were washed for 5 minutes using 1x PBS thrice to remove the DAPI residues. About 500 uL of 4 % PFA was used to fix the cells for 1 hour followed by permeabilization

© COPYRIGHT UPM

with the perm-block solution of 0.2 % Triton-X (1% BSA in 1x PBS) for 30 minutes. The cells were incubated with 200 uL of FITC conjugated TUJ1 (rabbit anti-mouse) antibody (1:1000 dilution) at 4°C overnight. The primary antibody was collected into perm-block solution and rinsed thrice with 1x PBS. About 200uL of goat anti-rabbit (1:1000 dilution) was added and incubated for 1 hour. The solution was rinsed 3 times with 1x PBS. The nuclei were counterstained with 200uL of 1ug/mL DAPI (1:10,000 dilution) for 10 minutes in 1 x PBS with 0.1% Triton-X. The stain was removed and washed with 1 x PBS about thrice. The PBS solution was removed entirely before removing the coverslip. A drop of mounting medium was added onto the slide and the coverslip was placed on top of the cells. Forceps was used to lift the coverslip from the well-plates. The slides were dried overnight at 4 °C. The next day, the coverslips were coated with nail polish and dried. The slides were observed under the microscope.

3.4 Fluorescent microscopy

The slides were placed on the stage of an Olympus BXL-50 fluorescence microscope and the appropriate filter was chosen (DAPI or FITC). The cells were observed under 10x magnification. Using the image analysis software (LIS analysis), six randomly selected fields from each slide were photographed.

© COPYRIGHT UPM

3.5 NeurphologyJ

NeurphologyJ, is capable of automatically quantifying neuronal morphologies such as soma number and thickness, neurite size, neurite endpoints, and attachment points from large volumes of 2D fluorescent images produced on the screen.

3.5.1 Installation Instruction

ImageJ (version 1.43) acts as an image processing and analytics tool whereas NeurphologyJ is an ImageJ plugin that quantifies neuronal morphologies. ImageJ was downloaded as a zip-file. The contents of the file were unzipped and stored in the ImageJ folder named “plugins” (default-c:\program files\ImageJ\plugins). Another plugin from ImageJ known as "particle remover" was downloaded from the following website: (http:/rsb.info.nih.gov / ij / plugins / particleremover.html). After this step, the NeurphologyJ option could be now be seen under the plugin menu when ImageJ was started.

3.5.2 Operation Instruction: NeurphologyJ interactive

The fluorescent stained images (10X magnification) were uploaded through the NeurphologyJ plugin (Figure 3.2).

© COPYRIGHT UPM

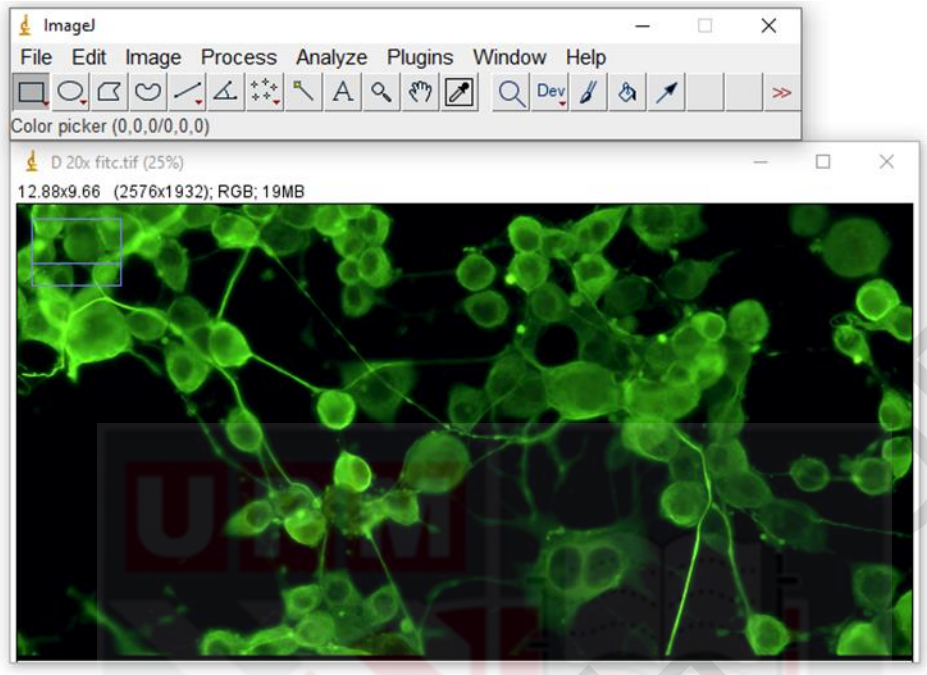

Figure 3.2: Fluorescent image of N2a cells after uploading in NeurphologyJ.

Under the 'Analyze' section of the menu, the images were converted to 12 bits to 16 bits. The image was now transformed into gray-scale (Figure 3.3). NeurphologyJ processed the input fluorescent image into a gray-scale image as the output with appropriate textures and enhanced features.

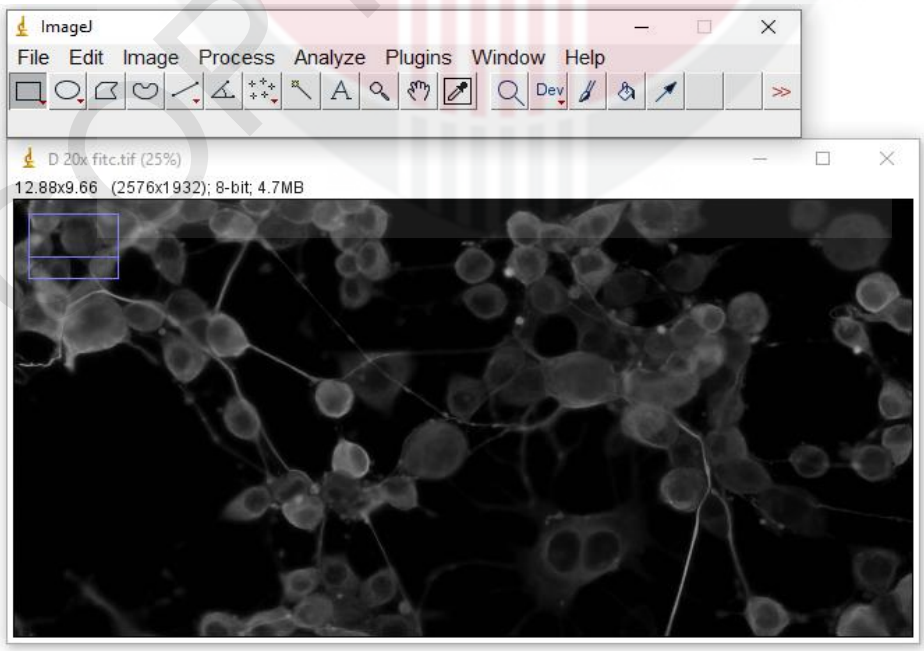

Figure 3.3: Gray-scale image of N2a cells after conversion using NeurphologyJ.

The gray-scale image was saved under TIFF format in a separate file (Figure 3.4).

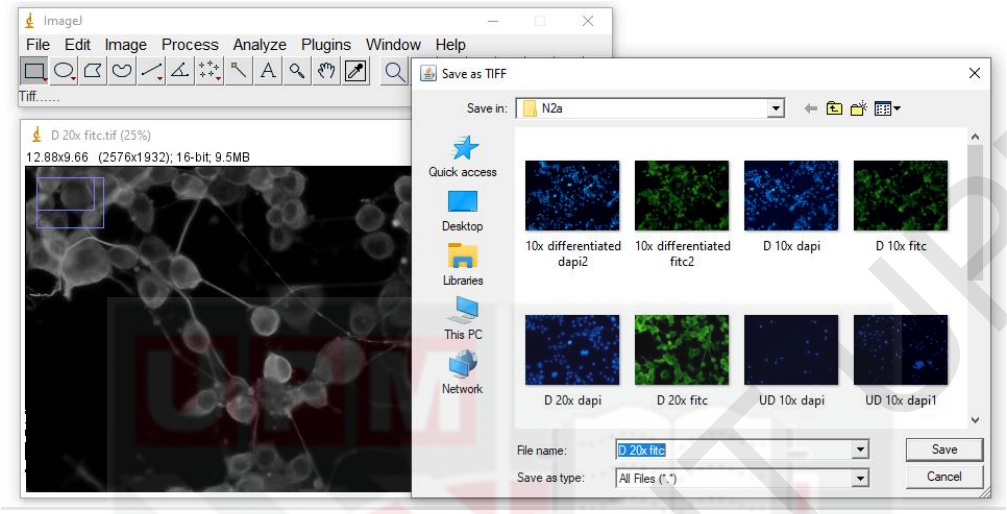

Figure 3.4: TIFF-formatted, gray-scale image of N2a cells saved.

The saved image (with TIFF format) was re-uploaded into the NeurphologyJ plugin. A setup wizard for optimization of the image was displayed. In the first threshold selection window, the "dark background" option was selected. The selection bar at the top was changed to select all the neurites (Figure 3.5). The optimal threshold was achieved by adjusting the bars with high and low threshold values.

© COPYRIGHT UPM

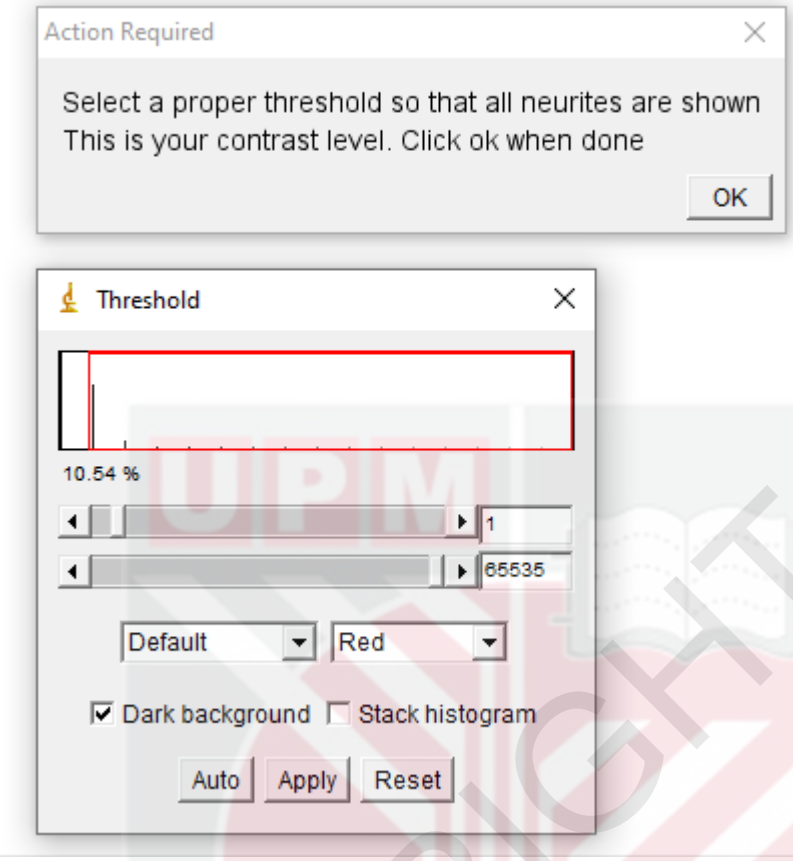

Figure 3.5: Adjustment of lower and upper selection bars to achieve optimum threshold levels.

© COPYRIGHT UPM

The image analyzed had higher neuron bodies pixel intensities, and lower neurite extremity intensities (Figure 3.6). Higher threshold value from the background image captured skipped fragments of the neurite by using the first threshold. The initial threshold value accurately identified boundaries of the cell body and initial segments of the neurite while the second threshold value showed better neurite extent. Neurite bodies and neurites were differentiated by applying a morphological opening with the resulting objects considered to be neuron bodies and the removed objects identified as neurites to the initial segmentation. The lower threshold was created with large second masks which contained and formed halos around the initial cell body masks. These halos hindered newly discovered parts of neurite from interacting with internal cell bodies.

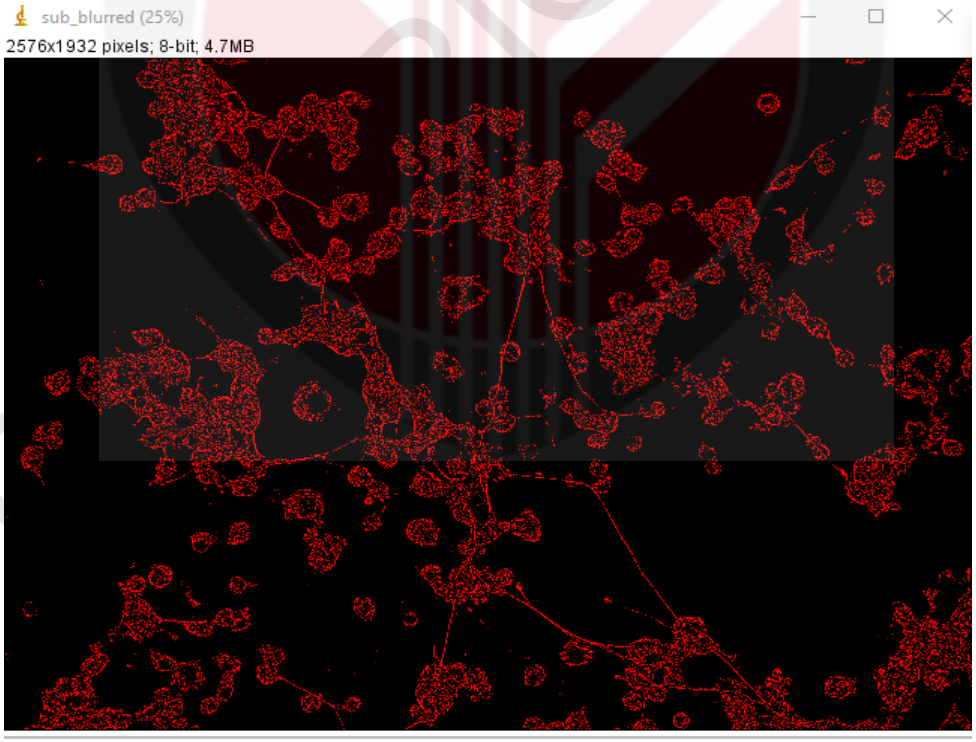

Figure 3.6: Output image of N2a cells after optimal threshold adjustment.

The optimum threshold level for the cell body was selected using the upper selection bar (Figure 3.7).

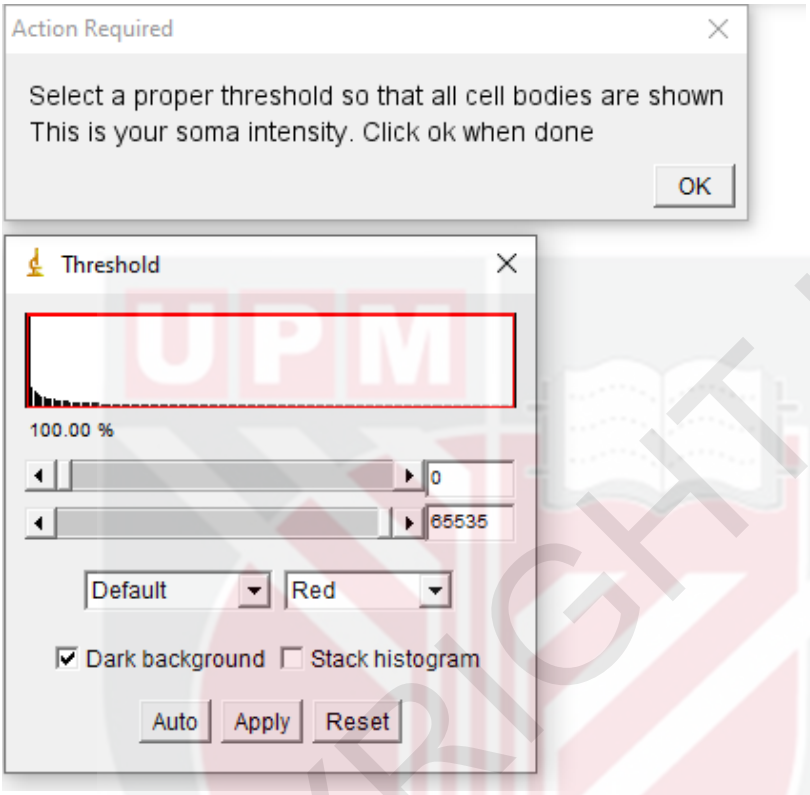

Figure 3.7: Adjustment of lower and upper selection bars to achieve optimum soma threshold levels.

After setup wizard was completed, the option for "contrast level" was shown in the window. The level was added based on the log window shown (Figure 3.8).

© COPYRIGHT UPM

.

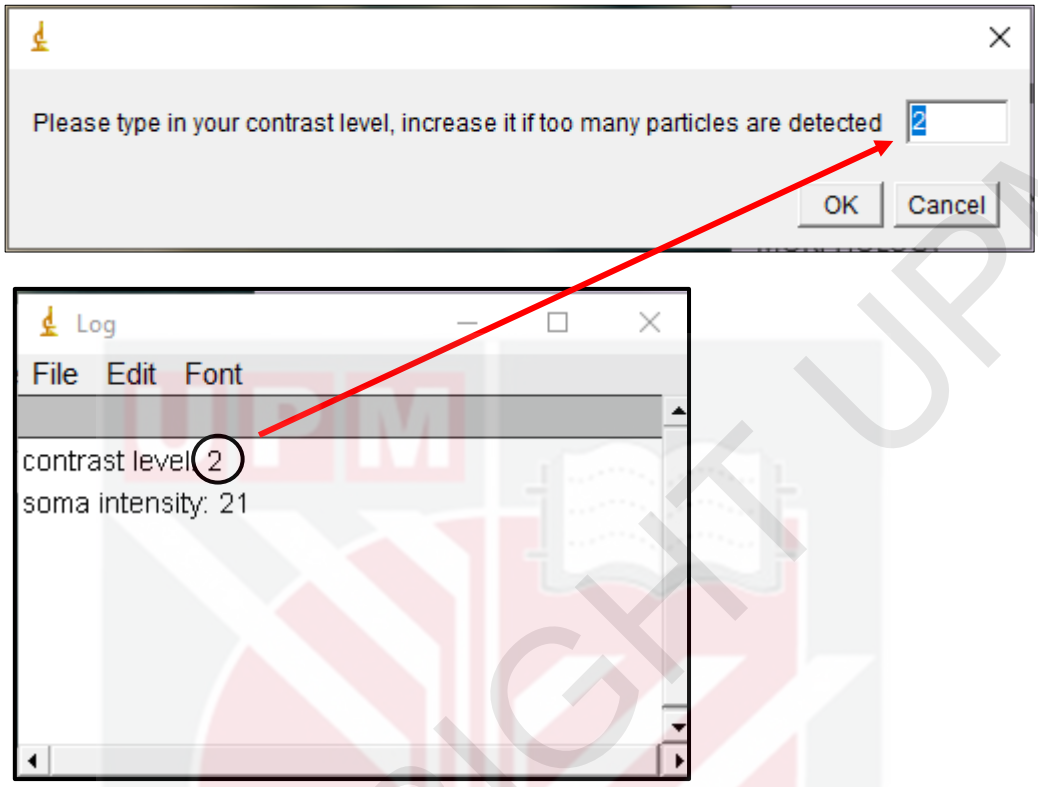

Figure 3.8: Adjustment of the contrast level.

The soma intensity algorithm was shown next. The value of soma intensity was added based on the value shown in the log window (Figure 3.9).

© COPYRIGHT UPM

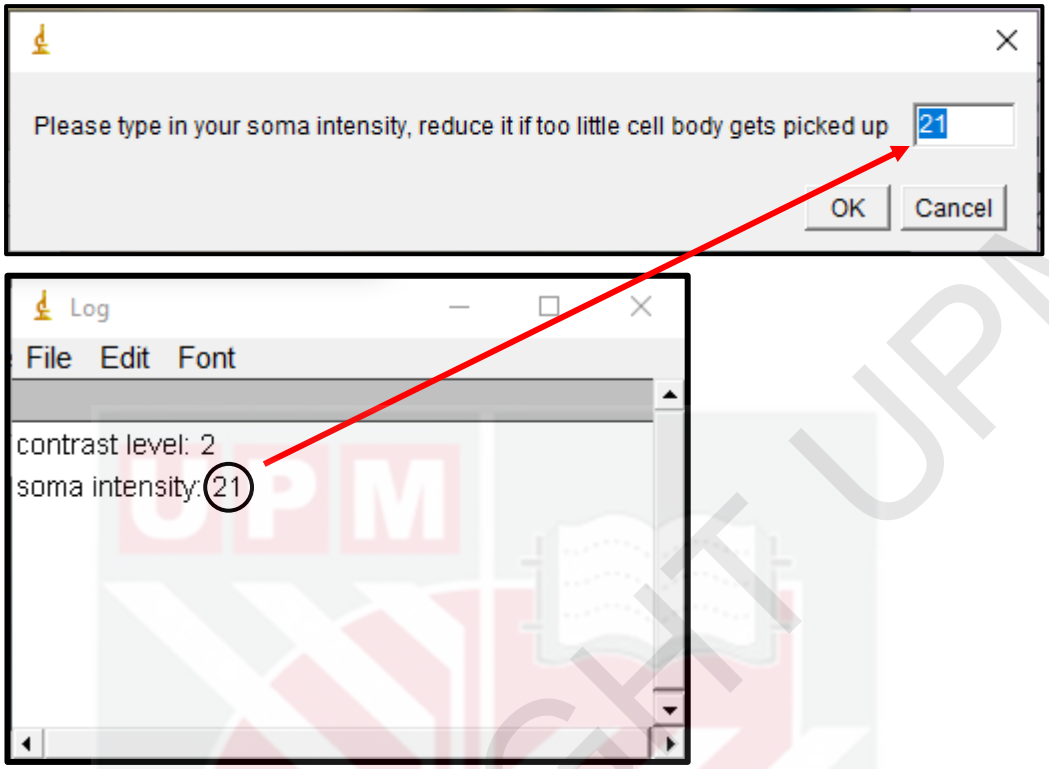

Figure 3.9: Adjustment of the soma intensity.

The neurite width adjustment panel was displayed in the next window. The displayed value can either be maintained or changed accordingly (Figure 3.10).

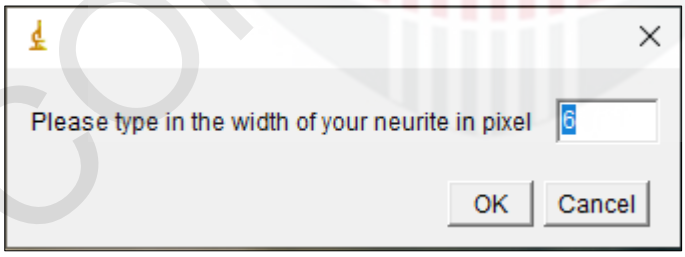

Figure 3.10: Adjustment of neurite width.

© COPYRIGHT UPM

The final user-defined window requested the "particle clean up value" (Figure 3.11). This value (in pixels) was determined by the maximum particle size to be extracted from the images. For larger objects, the value was increased.

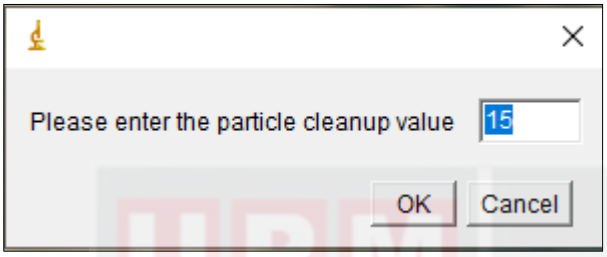

Figure 3.11: Adjustment of particle clean up value.

An opening for a reasonable threshold emerged. The upper selection bar was adjusted until no pixel counts fell within the region (Figure 3.12). The exact selection bar location didn't matter as long as it was without pixel counts in the field.

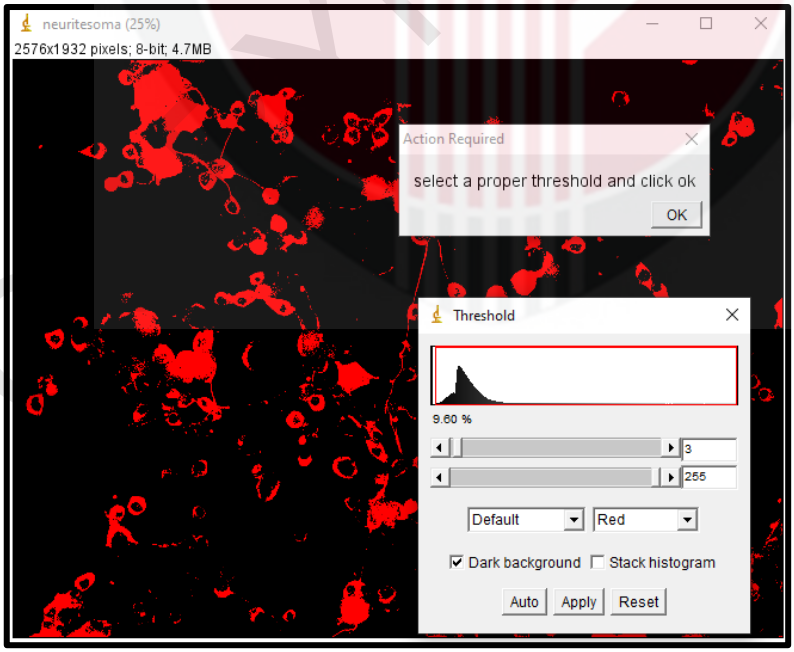

Figure 3.12: Adjustment of proper threshold selection values.

The last phase of NuerphologyJ, along with a summary table, generated 3 image windows and operation (Figure 3.13). The header displayed the analysed morphological parameters. The various morphological parameters in the pixel unit were analysed under the column "total area." NeurphologyJ quantifies morphological parameters based on the whole image field. To deduce the average neurite length per neuron, the parameter "neurite length" was separated by the parameter "soma." The parameter "neurite" measured the total area covered by the neurites while the parameter "neurite length" measured the neurite length. The neurite width was derived by dividing the parameter "neurite" with the parameter "neurite length".

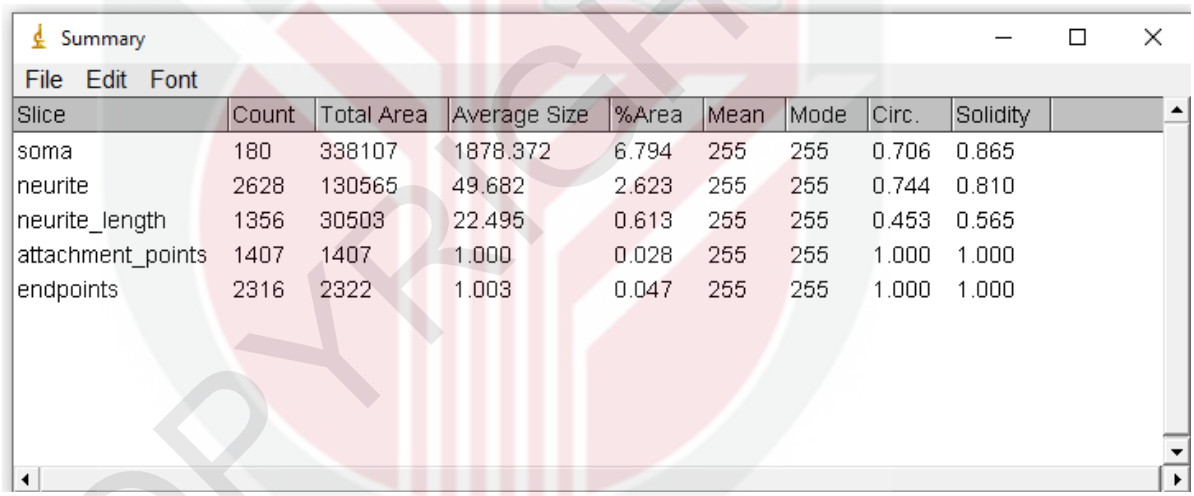

Slice	Count	Total Area	Average Size	%Area	Mean	Mode	Circ.	Solidity
soma	180	338107	1878.372	6.794	255	255	0.706	0.865
neurite	2628	130565	49.682	2.623	255	255	0.744	0.810
neurite_length	1356	30503	22.495	0.613	255	255	0.453	0.565
attachment_points	1407	1407	1.000	0.028	255	255	1.000	1.000
endpoints	2316	2322	1.003	0.047	255	255	1.000	1.000

Figure 3.13: Summary table of output from NeurphologyJ analysis.

© COPYRIGHT UPM

3.6 Statistical Analysis

In statistical analysis GraphPad Prism (version 8.0.2) was used. The difference in the means of neuronal morphologies for differentiated and undifferentiated N2a cells were designed using the Mann – Whitney test. A p-value of less than 0.05 was considered significant.

© COPYRIGHT UPM

CHAPTER 4

RESULTS

4.1 Fluorescent microscope images

Figure 4.1 shows the images of undifferentiated N2a cells whereas Figure 4.2 shows differentiated N2a cells (with serum deprivation). Fewer amounts of neurite outgrowths were observed in undifferentiated cells compared to the differentiated cells.

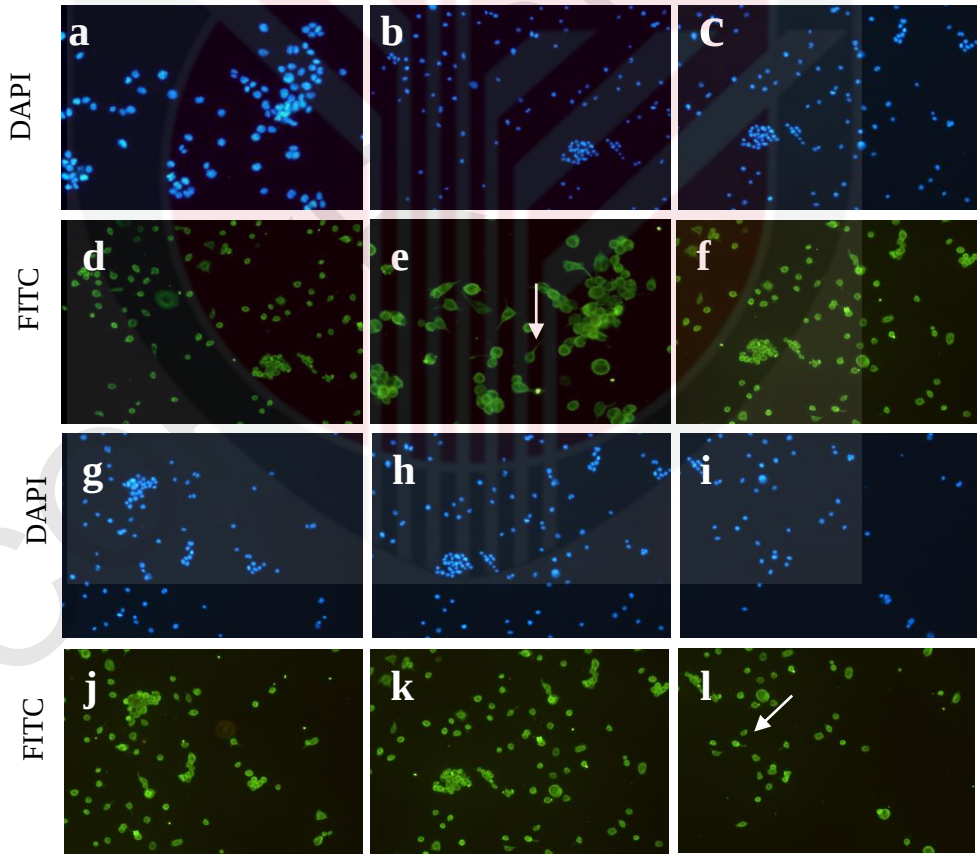

Figure 4.1: Immunocytochemical staining of untreated N2a cells as control. (a) (b) (c) (g) (h) (i). DAPI stains for nuclei blue. While, (d) (e) (f)(j) (k) (l) is the TUJ1 conjugated with FITC stains neuronal cells green. Arrows indicate neurite outgrowth. Photomicrographs of representative microscope fields were taken with a 10 x objective lens.

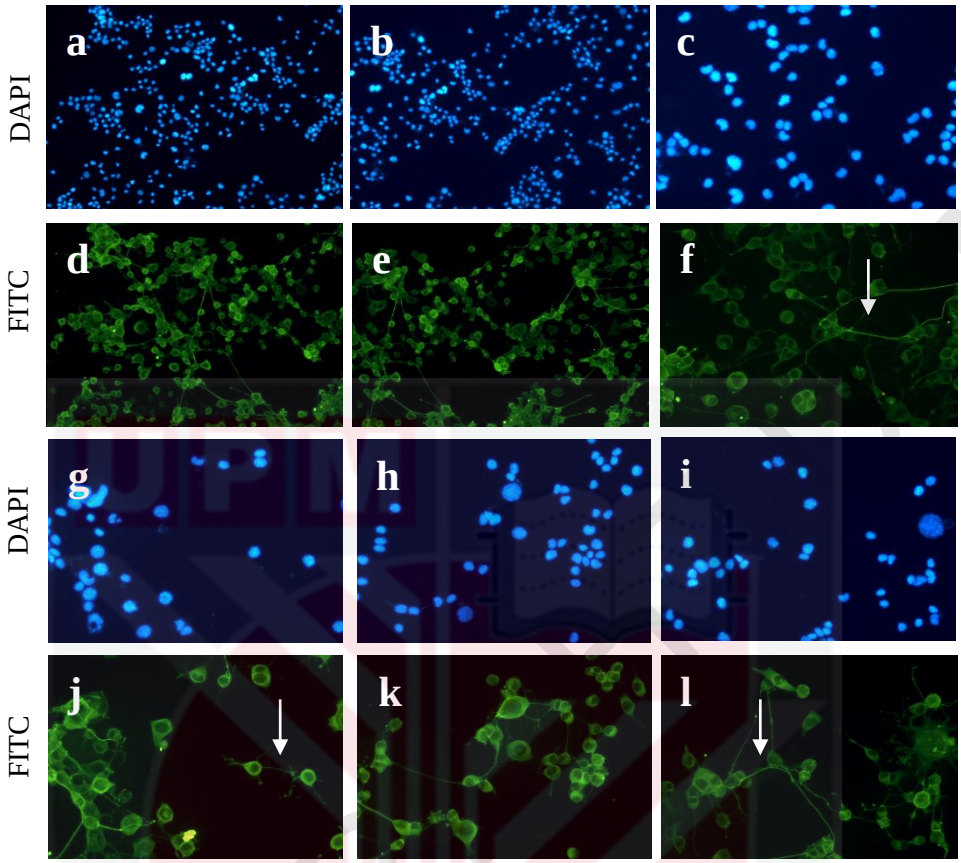

Figure 4.2: Immunocytochemical staining of treated cells N2a with serum deprivation. (a) (b) (c) (g) (h) (i). DAPI stains for nuclei blue. While, (d) (e) (f)(j) (k) (l) is the TUJ1 conjugated with FITC stains neuronal cells green. Arrows indicate neurite outgrowth. Photomicrographs of representative microscope fields were taken with a 10× objective lens.

© COPYRIGHT UPM

4.2 Digital analysis using NeurphologyJ

Figure 4.3 shows the mean soma count in N2a cells. The differentiated cells have higher soma counts than undifferentiated cells (88.50 ± 23.81 vs 161.33 ± 64.96). This difference between the means was found to be statistically significant ($p = 0.041$). Figure 4.4 shows the mean neurite count in N2a cells. The differentiated cells have higher neurite count than undifferentiated cells (772.00 ± 248.01 vs 2362.33 ± 605.43). This discrepancy was found to be statistically important between the tests ($p = 0.002$). Figure 4.5 shows the mean neurite length in N2a cells. The differentiated cells have higher neurite length than undifferentiated cells (2348.67 ± 1345.79 vs 18451.33 ± 7963.13). This difference was found statistically significant ($p = 0.002$) between the means. Figure 4.6 shows the mean attachment point in N2a cells. The differentiated cells have higher attachment point than undifferentiated cells (185.83 ± 90.95 vs 995.67 ± 295.88). This disparity was found to be statistically significant ($p = 0.002$) between ways. Figure 4.7 shows the mean endpoint point in N2a cells. The differentiated cells have higher endpoint point than undifferentiated cells (166.33 ± 85.77 vs 1383.50 ± 622.28). This discrepancy was found to be statistically important between the tests ($p = 0.002$).

© COPYRIGHT UPM

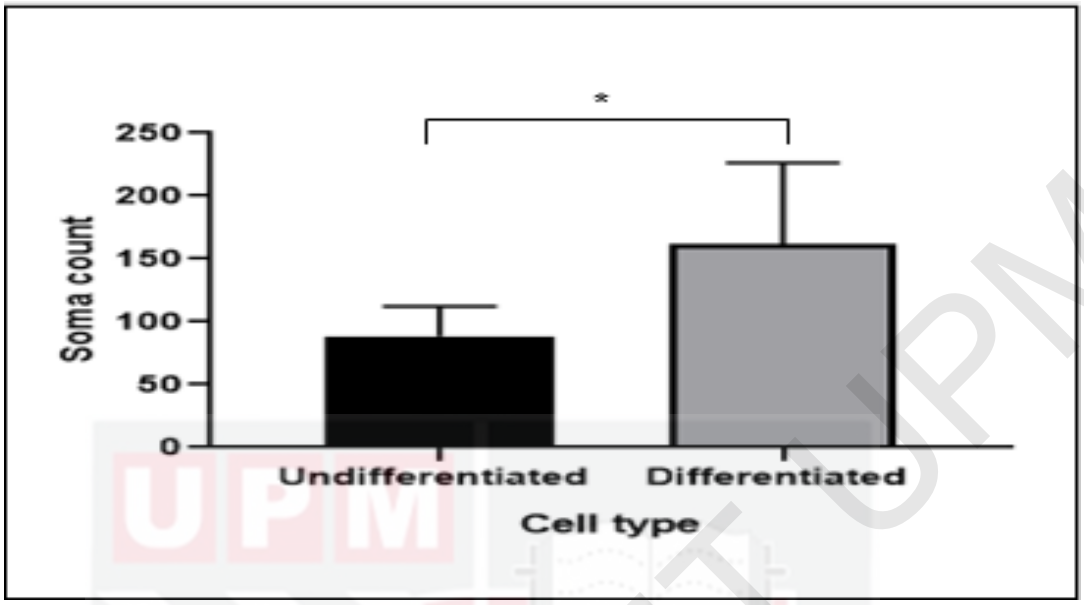

Figure 4.3: Mean soma count in N2a cells. The results are expressed as the mean counts obtained from six replicates of microscopic fields ± SD. * indicates statistically significant differences ($P < 0{\cdot}05$).

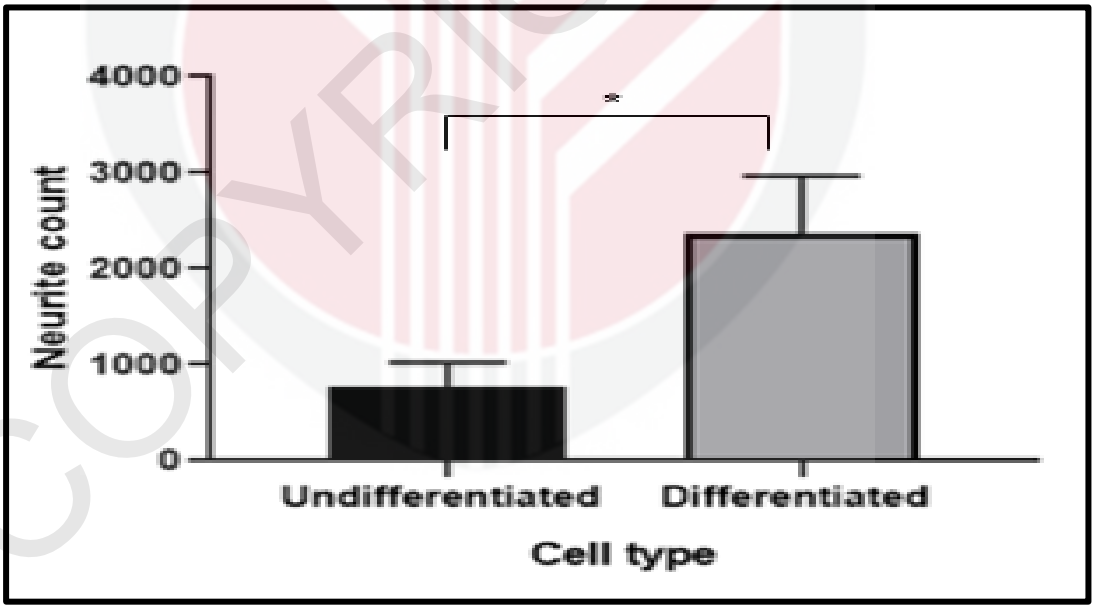

Figure 4.4: Mean neurite count in N2a cells. The results are expressed as the mean counts obtained from six replicates of microscopic fields ± SD.* indicates statistically significant differences ($P < 0{\cdot}05$).

© COPYRIGHT UPM

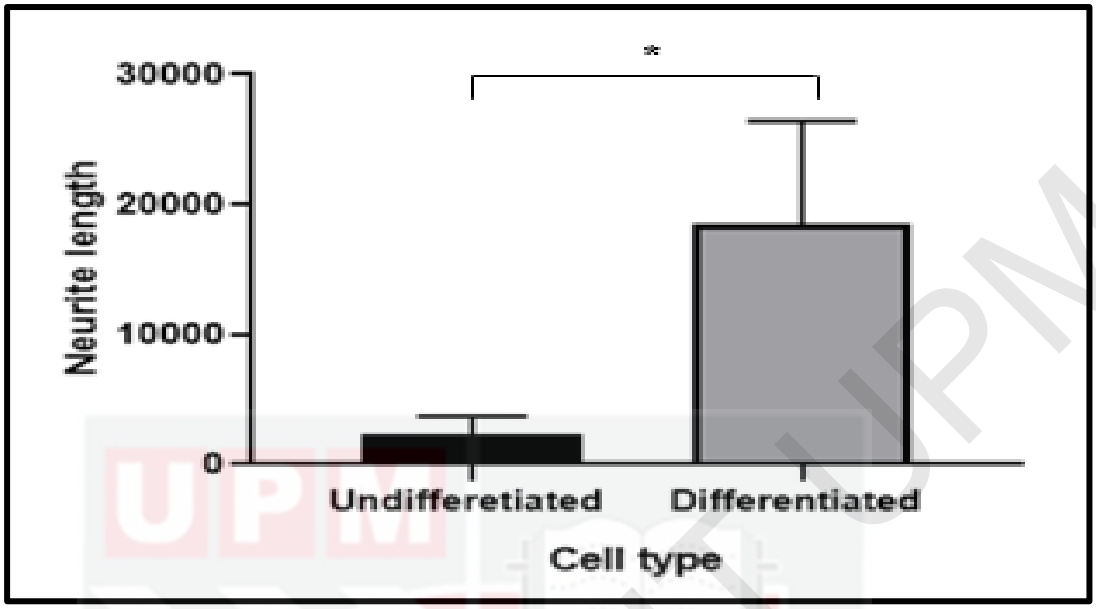

Figure 4.5: Mean neurite length in N2a cells. The results are expressed as the mean counts obtained from six replicates of microscopic fields ± SD.* indicates statistically significant differences (P < 0·05).

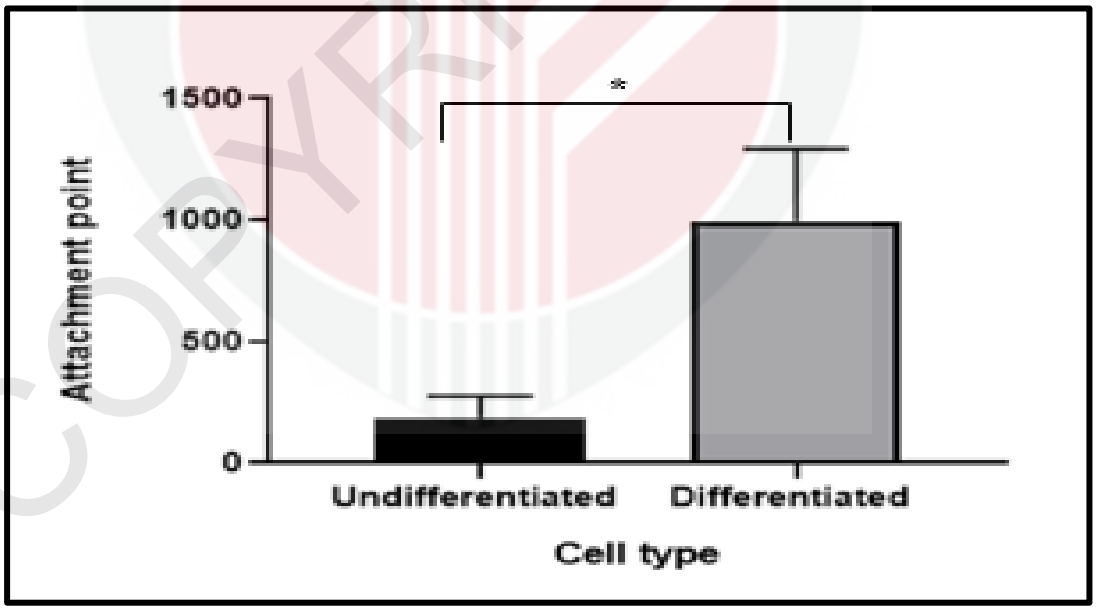

Figure 4.6: Mean attachment point in N2a cells. The results are expressed as the mean counts obtained from six replicates of microscopic fields ± SD.* indicates statistically significant differences (P < 0·05).

© COPYRIGHT UPM

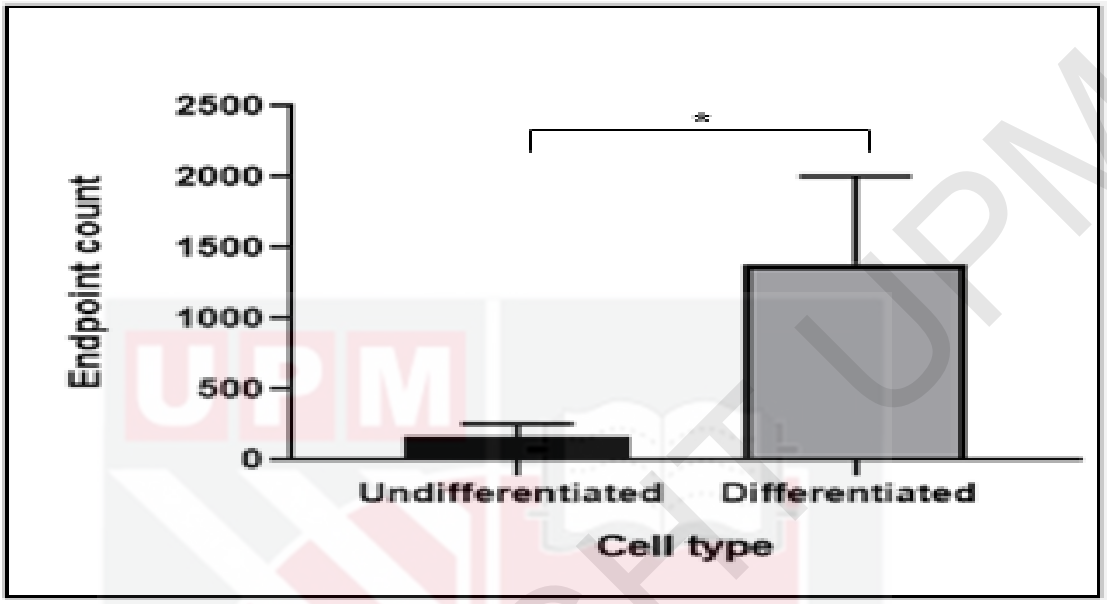

Figure 4.7: Mean endpoint point in N2a cells. The results are expressed as the mean counts obtained from six replicates of microscopic fields ± SD. * indicates statistically significant differences ($P < 0{\cdot}05$).

© COPYRIGHT UPM

CHAPTER 5

DISCUSSION

In recent years, high content screens have revolutionized biological studies of cells by providing a statistically relevant and quantitative basis for phenotypical observations. In line with this, the neuronal maturation moved from the processing of the images to the automated and unbiased study of the image data sets. In the context of neuronal regeneration studies, several automated image processing pipelines were developed which accurately quantify the characteristic changes in the N2a cell. Yet most existing methods show limited performance for well-connected and separated neuronal networks (Nadadhur *et al.*, 2019). Nevertheless, N2a cell is a useful model for investigating neuronal differentiation in the psychological factors, requiring a careful analysis. In order to meet this need, we explored NeurphologyJ to allows automatic neurite tracing in both undifferentiated and differentiated images. In the process of development, precision, speed compared with the sage of manual reconstruction and broad applicability of algorithms to specific data sets as performance parameters compared with other works (Sánchez *et al.*, 2019). In the neuroinflammation group the use of NeurphologyJ software to classify and analyze the morphological characteristics of the N2a cell has not been explored.

The maturation of the N2a cells was calculated using the conjugation of DAPI and FITC with different secondary antibodies. Based on our findings, differentiated cells showed significantly higher ($p<0.05$) soma counts, neurite counts, neurite length,

© COPYRIGHT UPM

attachment point and endpoint compared with undifferentiated cells. This follows on from previous research (Ramm *et al*, 2003 & Lejri *et al*, 2019). While current studies will benefit from higher sample counts and more research, these data nevertheless indicate the potential for using NeurphologyJ software as an alternative method to characterize N2a cells' morphological characteristics; between undifferentiated and differentiated N2a cells. Using the NeurphologyJ program will not only reduce human error and encourage analytical precision in contrast with the manual method but also save valuable research time. Quantification of N2a cell, using an image analysis method based on software, is an important feature of neural maturation studies. It is because it can provide knowledge about neural development which is useful for understanding neuronal morphological characteristics. N2a cells stained with FITC conjugated labelled TUJ1 antibody display certain variations in the length of the neurite and the branching between the differentiated and undifferentiated cells (Figures 4.1 - 4.2.).

Although this is qualitatively similar to the results recorded by Phan *et al.* (2013), this approach is not adequate to measure neuronal parameters such as soma count, attachment point and endpoint. In the following studies, Figures 4.3 and 4.7 provided an example of NeurphologyJ production using N2a cells according to the parameter. It can be shown that NeurphologyJ measure the parameters selected for both undifferentiated and differentiated N2a cells with success. In NeurphologyJ many other studies quantified these parameters using certain cell types, such as primary cortical neurons and pluripotent stem cells induced by humans (iPSC) (An, B *et al.* ,2015; Nadadhur, Long *et al.*, 2017). In general, nondifferentiated cells have lower

© COPYRIGHT UPM

soma and neurite numbers, shorter distances, fewer attachments, and endpoints. The findings of this analysis showed that the mean values of differentiated N2a cells are

significantly higher than the undifferentiated N2a cells. This means that NeurphologyJ will decide exactly the predicted morphological differences between the undifferentiated and the differentiated cells.

NeurphologyJ shows strong tracking in tracing of neurites and segmentation of somas under culture conditions, neurite research in cultures grown for up to 23 days. The software supported the identification of subtle neural network modifications at various rates (neuron count, neurite length, soma count, attachment points and endpoints), especially at the thin neurite level; where it has low fluorescence strength relative to the remaining networks. NeurphologyJ worked better on various sets of image data that were taken at different resolutions and was sensitive despite relative high noise levels (Shariff *et al.*, 2010). Using the program, we found that neurites spread rapidly until it reaches the stage of appropriate connectivity, after which the neuronal network grows slowly, consistent with previous results. There are still improvements that can be made regarding processing speed or performance in segmentation. For example, solutions might be implemented to prevent or recover erroneous nuclei separation caused by the watershed algorithm. That could be achieved by re-joining posteriori or model fitting based on a library of predicted shapes. The use of NeurphologyJ is promising in neurological research to estimate subtle changes in long-term neuronal cultures used as an in vitro mature nervous system model. It is recognized that neurological disease as well as environmental events such as exposure to toxic compound or radiation, can trigger cognitive impairment and memory loss in

© COPYRIGHT UPM

adults (Ossinger *et al.*, 2020). Both in vivo and in vitro experiments have shown that low- or high-dose ionizing radiation causes neuronal death.

Valuable efforts have recently been made to permit neuronal network segmentation in 3D. Several algorithms have been developed, one of which sequentially detects the neurite centre line and fuses individual branches into trees to reconstruct 3D neurons and one based on 3D open-curve active contours to track and reconstruct neurites (Li *et al.*, 2017). While these methods demonstrate good efficiency and high precision in the reconstruction of individual neurons, these algorithms include high resolution and lower resolution images computation capacity, making them less suitable for applications with high quality at this point. Neither do all applications require this amount of knowledge. The goal of much high content and high-throughput screening reliable phenotypic biological effect indicator (Chiola *et al.*, 2019). Neuronal network density is something we've seen from parameters, which can be easily measured in 2D and can therefore be implemented with much lower computational requirements and higher global performance in such screening.

© COPYRIGHT UPM

CHAPTER 6

CONCLUSION AND FUTURE RECOMMENDATIONS

The undifferentiated and differentiated cells shows morphological changes after the culture with and without serum deprivation. Meanwhile, the differentiated cell has more neurite outgrowth and branching. The undifferentiated and differentiated cells can be quantified using NeurphologyJ on the parameters given. Therefore, it was observed that differentiated and undifferentiated N2a cells had separate neuronal outgrowths. Such results suggest that the program NeurphologyJ can be useful for measuring the morphological characteristics of both undifferentiated and differentiated N2a cells. Using the freeware tool NeurphologyJ allows to quantify soma number, neurite number, neurite length, attachment point, and end point quickly, accurately and objectively. NeurphologyJ provides the benefit of quantifying single neurite lengths and analyzing clustered nuclei. This software has proven useful as a toolbox for neuronal quantification.

For future applications, N2a cells differentiated using other types of methods may be conducted for a better understanding of cell maturation parameters. Other than that, a comparison of N2a cells with other neuronal cell lines by measuring the parameters using NeurphologyJ software can also be conducted. Future analysis would also benefit from a larger sample size as greater statistical power can achieved to better represent the data in the targeted population.

© COPYRIGHT UPM

REFERENCES

An, B., Tang-Schomer, M. D., Huang, W., He, J., Jones, J. A., Lewis, R. V., & Kaplan, D. L. (2015). Physical and biological regulation of neuron regenerative growth and network formation on recombinant dragline silks. *Biomaterials*, *48*, 137-146.

Barnes, A. P., & Polleux, F. (2009). Establishment of axon-dendrite polarity in developing neurons. *Annual review of neuroscience*, *32*.

Chen, Y. J., Huang, Y. A., Ho, C. T., Yang, J. M., Chao, J. I., Li, M. C., & Hwang, E. (2020). miR6236, a microRNA suppressed by the anisotropic surface topography, regulates neuronal development and regeneration. *bioRxiv*.

Chiola, S., Santo, M., & Mallamaci, A. (2019). Intraventricular Transplantation of Engineered Neuronal Precursors for In Vivo Neuroarchitecture Studies. *JoVE (Journal of Visualized Experiments)*, (147), e59242.

Chiola, S., Santo, M., & Mallamaci, A. (2019). Intraventricular Transplantation of Engineered Neuronal Precursors for In Vivo Neuroarchitecture Studies. *JoVE (Journal of Visualized Experiments)*, (147), e59242.

Djouhri, L., Zeidan, A., & Abd El-Aleem, S. A. (2020). Changes in expression of Kv7. 5 and Kv7. 2 channels in Dorsal Root Ganglion Neurons in the Streptozotocin Rat Model of Painful Diabetic Neuropathy. *Neuroscience Letters*, 135277.

El Merhie, A., Salerno, M., Toccafondi, C., & Dante, S. (2019). Neuronal-like response of N2a living cells to nanoporous patterns of thin supported anodic alumina. *Colloids and Surfaces B: Biointerfaces*, *178*, 32-37.

© COPYRIGHT UPM

Ho, S. Y., Chao, C. Y., Huang, H. L., Chiu, T. W., Charoenkwan, P., & Hwang, E. (2011). NeurphologyJ: an automatic neuronal morphology quantification method and its application in pharmacological discovery. *Bmc Bioinformatics*, *12*(1), 1-18.

Lejri, I., Agapouda, A., Grimm, A., & Eckert, A. (2019). Mitochondria-and oxidative stress-targeting substances in cognitive decline-related disorders: from molecular mechanisms to clinical evidence. *Oxidative Medicine and Cellular Longevity*, *2019*.

Li, Y., Cao, J., Chen, M., Li, J., Sun, Y., Zhang, Y., Zhu, Y., Wang, L. and Zhang, C. (2017). Abnormal neural progenitor cells differentiated from induced pluripotent stem cells partially mimicked development of TSC2 neurological abnormalities. *Stem cell reports*, *8*(4), 883-893.

Long, B.L., Li, H., Mahadevan, A., Tang, T., Balotin, K., Grandel, N., Soto, J., Wong, S.Y., Abrego, A., Li, S. and Qutub, A.A. (2017). GAIN: A graphical method to automatically analyze individual neurite outgrowth. *Journal of neuroscience methods*, *283*, 62-71.

Mitra, J., Jain, S., Sharma, A., & Basu, B. (2013). Patterned growth and differentiation of neural cells on polymer derived carbon substrates with micro/nano structures in vitro. *Carbon*, *65*, 140-155.

Nadadhur, A.G., Alsaqati, M., Gasparotto, L., Cornelissen-Steijger, P., van Hugte, E., Dooves, S., Harwood, A.J. and Heine, V.M., (2019). Neuron-glia interactions increase neuronal phenotypes in tuberous sclerosis complex patient iPSC-derived models. *Stem cell reports*, *12*(1), 42-56.

Ossinger, A., Bajic, A., Pan, S., Andersson, B., Ranefall, P., Hailer, N. P., & Schizas, N. (2020). A rapid and accurate method to quantify neurite outgrowth from cell and tissue cultures: Two image analytic approaches using adaptive thresholds or machine learning. *Journal of Neuroscience Methods*, *331*, 108522.

© COPYRIGHT UPM

Phan, C. W., David, P., Naidu, M., Wong, K. H., & Sabaratnam, V. (2013). Neurite outgrowth stimulatory effects of culinary-medicinal mushrooms and their toxicity assessment using differentiating Neuro-2a and embryonic fibroblast BALB/3T3. *BMC Complementary and Alternative Medicine*, *13*(1), 261.

Pu, J., Gao, T., Zheng, R., Fang, Y., Ruan, Y., Jin, C., Shen, T., Tian, J. and Zhang, B., (2020). Parkin mutation decreases neurite complexity and maturation in neurons derived from human fibroblasts. *Brain Research Bulletin*.

Radio, N. M., & Mundy, W. R. (2008). Developmental neurotoxicity testing in vitro: models for assessing chemical effects on neurite outgrowth. *Neurotoxicology*, *29*(3), 361-376.

Ramm, P., Alexandrov, Y., Cholewinski, A., Cybuch, Y., Nadon, R., & Soltys, B. J. (2003). Automated screening of neurite outgrowth. *Journal of biomolecular screening*, *8*(1), 7-18.

Rueden, C. T., Schindelin, J., Hiner, M. C., DeZonia, B. E., Walter, A. E., Arena, E. T., & Eliceiri, K. W. (2017). ImageJ2: ImageJ for the next generation of scientific image data. *BMC bioinformatics*, *18*(1), 529.

Sánchez-Vidaña, D.I., Po, K.K.T., Fung, T.K.H., Chow, J.K.W., Lau, W.K.W., So, P.K., Lau, B.W.M. and Tsang, H.W.H., (2019). Lavender essential oil ameliorates depression-like behavior and increases neurogenesis and dendritic complexity in rats. *Neuroscience letters*, *701*, 180-192.

Saroa, R., & Bagai, U. (2018). Evaluation of T cells infiltration inhibition in brain by immunohistochemistry during experimental cerebral malaria. *Journal of Parasitic Diseases*, *42*(4), 537-549.

Schindelin, J., Rueden, C.T., Hiner, M.C. and Eliceiri, K.W., (2015). The ImageJ ecosystem: An open platform for biomedical image analysis. *Molecular reproduction and development*, *82*(7-8), 518-529.

© COPYRIGHT UPM

Shariff, A., Kangas, J., Coelho, L. P., Quinn, S., & Murphy, R. F. (2010). Automated image analysis for high-content screening and analysis. *Journal of biomolecular screening*, *15*(7), 726-734.

West, A. E., & Greenberg, M. E. (2011). Neuronal activity–regulated gene transcription in synapse development and cognitive function. *Cold Spring Harbor perspectives in biology*, *3*(6), a005744.

Wu, J., Kong, F., Pan, Q., Du, Y., Ye, J., Zheng, F., Li, H. and Zhou, J., (2017). Autophagy protects against cholesterol-induced apoptosis in pancreatic β-cells. *Biochemical and biophysical research communications*, *482*(4), 678-685.

© COPYRIGHT UPM

APPENDIX A

Mann-Whitney test (soma count)

p-value	0.0411
Exact or approximate P value?	Exact
P value summary	*
Significantly different (P < 0.05)?	Yes
One- or two-tailed P value?	Two-tailed
Sum of ranks in column undifferentiated, differentiated	26, 52
Mann-Whitney U	5

Mann-Whitney test (neurite count)

p-value	0.0022
Exact or approximate P value?	Exact
P value summary	**
Significantly different (P < 0.05)?	Yes
One- or two-tailed P value?	Two-tailed
Sum of ranks in column undifferentiated, differentiated	21, 57
Mann-Whitney U	0

© COPYRIGHT UPM

Mann-Whitney test (neurite length)

p-value	0.0022
Exact or approximate P value?	Exact
P value summary	**
Significantly different (P < 0.05)?	Yes
One- or two-tailed P value?	Two-tailed
Sum of ranks in column undifferentiated, differentiated	21, 57
Mann-Whitney U	0

Mann-Whitney test (attachment point)

p-value	0.0022
Exact or approximate P value?	Exact
P value summary	**
Significantly different (P < 0.05)?	Yes
One- or two-tailed P value?	Two-tailed
Sum of ranks in column undifferentiated, differentiated	21, 57
Mann-Whitney U	0

© COPYRIGHT UPM

Mann-Whitney test (endpoints)

p-value	0.0022
Exact or approximate P value?	Exact
P value summary	**
Significantly different (P < 0.05)?	Yes
One- or two-tailed P value?	Two-tailed
Sum of ranks in column undifferentiated, differentiated	21, 57
Mann-Whitney U	0

© COPYRIGHT UPM